does indeed become somewhat worse if the system is not allowed to attain equilibrium, the extent of the deterioration is not as pronounced as generally assumed, and the rate of changes in the thermodynamic conditions does obviously not play a decisive role.

The reason for this behavior lies in particular mechanisms of the nonequilibrium processes, which act in a favorable direction: As shown in Figure 8, long chains are preferentially incorporated in the ne gel, in a similar manner as they would be in equilibrium experiments at a somewhat lower temperature. With respect to fractionation, the effect is, however, not totally equivalent. This is due to the fact that the amount of material captured in the ne gel (cf. eq 6) increases linearly with the logarithm of the chain length, whereas the mass ratio of the individual polymer molecules contained in the coexisting equilibrium phases increases exponentially[8] with that variable.

Finally, some speculations appear worthwhile to be mentioned, namely, some interesting implications of the present findings for the discussion of the processes taking place in the preparation of polymer blends. If two-phase mixtures of polymer A and polymer B are prepared starting from homogeneous systems (e.g. by changing the variables of state or by evaporating a solvent) and equilibrium cannot be reached, molecules of polymer A will be captured in the phase rich in B and vice versa. This means that the concentration profile in the interfacial region of the segregated particles will change as if some compatibilizer (like a copolymer of A and B) were added, and this should bear consequences concerning the mechanical properties of the blend.

Acknowledgment. The present work was sponsored within the scope of the SFB 262 by the "Deutsche Forschungsgemeinschaft". This support is gratefully acknowledged. Furthermore, we thank PSS (Mainz) for supplying polymer standards and D. A. Pärsch-Roos, K. Klink, A. Kohlbecher, and J. Kurtz for their assistance.

Registry No. PS, 9003-53-6; CH, 110-82-7; TD, 493-02-7.

References and Notes

(1) Baker, C. A.; Williams, R. J. P. *J. Chem. Soc.* **1956**, 2352.
(2) Geerissen, H.; Roos, J.; Wolf, B. A. *Makromol. Chem.* **1985**, *186*, 735.
(3) Ballauff, M.; Krämer, H.; Wolf, B. A. *J. Polym. Sci., Polym. Phys. Ed.* **1983**, *21*, 1217.
(4) Herold, F. Ph.D. Thesis, Johannes-Gutenberg-universität Mainz, 1985.
(5) Derham, K. W.; Goldsbrough, J.; Gordon, M. *Pure Appl. Chem.* **1974**, *38*, 97.
(6) Allegra, G.; Ganazzoli, F. *Gazz. Chim. Ital.* **1987**, *117*, 599.
(7) Daoud, M.; Cotton, J. P.; Farnoux, B.; Jannink, G.; Sarma, G.; Benoit, H.; Dublessix, R.; Picot, C.; de Gennes, P. G. *Macromolecules* **1975**, *8*, 804.
(8) Wolf, B. A.; Bieringer, H. F.; Breitenbach, J. W. *Br. Polym. J.* **1978**, *10*, 156.

Reptation in Semidilute Solutions of Wormlike Polymers

B. Tinland,[†] G. Maret,*[,‡] and M. Rinaudo[†]

Centre de Recherches sur les Macromolécules Végétales, CNRS, 53x, F-38041 Grenoble Cedex, France, and Hochfeld Magnetlabor, Max Planck Institut für Festkörperforschung, 166x, F-38042 Grenoble Cedex, France. *Received February 9, 1989*

ABSTRACT: We report fringe pattern fluorescence bleaching measurements of the self-diffusion coefficient of the wormlike polysaccharide xanthan at various molecular weights in aqueous solutions. Three distinguished concentration regimes are found: the dilute regime, the semidilute regime, and a new "concentrated" regime characteristic of wormlike polymers at concentrations where the intermolecular correlation length becomes smaller than the persistence length. We give simple scaling arguments that are consistent with the main trends in the data as a function of concentration and chain length and provide a fair estimate for the self-diffusion constant and the crossover concentrations.

Introduction

Understanding the motion of a polymer chain when surrounded by other (alike) polymer chains—such as occurring in semidilute polymer solutions or polymer melts—is of great fundamental and practical interest in polymer dynamics. Since the low-frequency rheological properties of such liquids are governed by the translational diffusion of the chains over distances large compared to the chain extension, much theoretical and experimental work has concentrated on the translational self-diffusion coefficient D_s measured on a macroscopic scale.[1-3] D_s depends on single-chain properties such as chain flexibility and chain length but also on interchain interactions and hence on the polymer concentration. In one of the prominent models proposed[4,5] to describe this a priori complex problem of statistical physics, one assumes that a given test chain "reptates" through the mess of surrounding chains. This means the test chain, being essentially confined at short times by the other chains into a curvilinear tube along its contour, has zero transverse diffusion and effectively propagates by one-dimensional diffusion along this contour. In the reptation model, predictions of D_s have been made for flexible chains in semidilute solutions and melts most easily by using simple scaling arguments.[6,7] The agreement with a large body of experimental data appears satisfactory now.[1] Reptation of rods has also been treated theoretically,[8-11] but a comparison with experiments appears

[†] Centre de Recherches sur les Macromolécules Végétales.
[‡] Max Planck Institut für Festkörperforschung.

0024-9297/67/2200-0596$02.50/0

difficult for the lack of truly rodlike polymer systems. Indeed, most real so-called stiff polymers can be considered rodlike only at short chain lengths, and are better approximated by weakly bending rods or wormlike chains[12-15] at the chain lengths typically used in experiments.[16-20] The flexibility, or rigidity, against bending is then characterized by the persistence length P. Since in the scaling approach for reptation one compares length scales, one expects a new regime[21] to appear for wormlike chains, which is not present for flexible chains or for rods.

In this paper we first outline the scaling arguments for wormlike chains. This provides expressions for D_s in the dilute, semidilute, and concentrated regime and for the corresponding crossover concentrations. The results are compared to recent predictions of D_s in the concentrated regime by Doi[14] and Semenov.[15] We then describe measurements of D_s on aqueous solutions of the semiflexible polysaccharide xanthan performed over the corresponding concentration (c) range at various chain lengths L, using the fringe pattern fluorescence bleaching technique.[21] We show that the experimental crossover concentrations and the dependence of D_s on L and c roughly agree with the simple scaling predictions; it turns out, however, that the experimentally accessible L and c range for this polysaccharide in water does not allow us to fully explore the limiting behavior in the different regimes.

Scaling Approach

Let us consider first a single wormlike polymer chain of contour length $L = Na$, N being the number of monomers and a the monomer length, and of persistence length P. If $L \ll P$ (and, of course, $a \ll L$) the chain is rodlike. On increasing L the chain becomes more and more a bending rod and ultimately ($L \gg P$) assumes conformations of a random coil. The mean-square radius of gyration $\langle R_{go}^2 \rangle$ of a wormlike chain (which is stiff on the monomeric length scale a, but not on a scale $\gg P$) is given by[23]

$$\langle R_{go}^2 \rangle = L^2\left[\frac{1}{3x} - \frac{1}{x^2} + \frac{2}{x^3} - \frac{2(1-e^{-x})}{x^4}\right] \quad (1)$$

with $x = L/P$. Equation 1 describes the crossover from rods ($x \to 0$) to Gaussian random coils ($x \to \infty$) with no excluded-volume effects. For long chains the overall average chain extension is governed by random walk statistics with a rigid statistical segment, the so-called "Kuhn segment" of length $2P$. In this limit the radius of gyration becomes

$$R_{go} = \langle R_{go}^2 \rangle^{1/2} = (2PL/6)^{1/2} \quad (2)$$

The mean-square end-to-end vector $\langle h^2 \rangle$ of the chain is $\langle h^2 \rangle = 2PL$. Note that this chain is much more extended than a flexible chain with statistical length a, for which $R_{go} = (aL/6)^{1/2}$.

The above assumption of ideal random walk allows interpenetration of chain segments, which is of course unphysical. When taking the excluded volume between segments into account[24,25] the overall chain extension increases by a factor of $\alpha_s(z)$

$$\langle R_g^2 \rangle = \alpha_s^2(z)\langle R_{go}^2 \rangle \quad (3)$$

$\alpha_s(z)$ depends on the excluded-volume parameter z, which is a function of L, P, and the excluded volume β between segments. Using for β the excluded volume[24] between two rodlike Kuhn segments of length $2P$ and diameter d_e (under the assumption $2P \gg d_e$), $\beta = 2\pi d_e P^2$, one obtains

$$z = (3/8\pi)^{3/2}2^{1/2}\pi d_e/P(L/P)^{1/2} \quad (4)$$

Excluded-volume effects are small when $z \ll 1$ or $(L/P)^{1/2} \ll P/d_e$. This study concerns polymers with 450 nm $< L <$ 9400 nm, $P \simeq 45$ nm, and $d_e \simeq 2.8$ nm.[26] Therefore this condition is not satisfied and chain extension should be taken into account, in principle. For very long chains ($z \to \infty$) the length exponent of R_g asymptotically becomes[27] 3/5 rather than 1/2. For finite lengths the chain expansion can be described by[24]

$$\alpha_s^2(z) = 0.541 + 0.459(1 + 6.04z)^{0.46} \quad (5)$$

Combining eq 1, 3, 4, and 5, we find that for our polymer system the effects of chain expansion are small ($\alpha_s \leq 1.08$) and the apparent length exponent of R_g (defined as $d(\log R_g)/d(\log L)$) lies between 0.6 and 0.53, just above the crossover region from rodlike to Gaussian chains. The Flory excluded-volume exponent 3/5 would be approached only for L values about 4 orders of magnitude higher than the highest L value studied. Therefore, in view of the approximate nature of the scaling approach discussed below, we shall neglect excluded-volume effects and use for R_g eq 2 in the semidilute and concentrated regime.

It is well-known that in the *dilute* concentration regime where interchain interactions are negligible the self-diffusion coefficient of a long ($L \gg P$) random coil polymer can be described by the Stokes–Einstein relation

$$D_s = kT/6\pi\eta_0 R_h \quad (6)$$

This defines the hydrodynamic radius R_h of an equivalent sphere. η_0 is the solvent viscosity, k the Boltzmann constant, and T the temperature. R_h is related to R_g by $R_h = \zeta R_g$ where the coefficient ζ is ≤ 1 and depends on the extent of penetration of solvent flow through the coil. For wormlike chains an approximate expression is[28]

$$\zeta = 3^{1/2}(1 + x/4)^{1/2}[27x/16 + \ln^2(3L/2d)]^{-1/2} \quad (7)$$

d is the effective hydrodynamic diameter of the chain segment. It is not necessarily equal to the effective excluded-volume diameter d_e.

With increase in the polymer concentration c, different chains progressively interpenetrate and the free Einstein diffusion picture becomes meaningless. The crossover concentration c^* for the onset of interchain interactions is usually estimated by the condition that the average distance between the centers of mass of the chains equals the average chain extension (of order R_g): At this concentration there is one chain per volume R_g^3

$$c^* = mL/R_g^3 \quad (8)$$

m is the mass per unit length of the polymer chain.

Above c^* the increasing number of entanglements reduces the probability for a given test coil to perform large-scale diffusion transverse to the direction of its local contour. Diffusion via reptation may become the dominant mechanism. Before treating the *semidilute* case, let us briefly recall the conceptually more straightforward scaling estimation of D_s for the reptation model in *melts* (i.e., *no* solvent). In this case transverse motions are forbidden on a short time scale. The chain diffuses back and forth along its contour inside a tube of diameter $\simeq d$ and length L. Only those parts of the chain near the ends that leave the initial tube are free to choose a new random path. This defines an average lifetime τ_R of the initial tube given by the time it takes the chain to perform *one-dimensional* diffusion over the distance L along its contour.

$$L^2 = 2D_{tube}\tau_R \quad (9)$$

D_{tube} is the curvilinear self-diffusion coefficient of the polymer parallel to the contour in a medium of effective viscosity η. If we neglect, for now, correction terms of order ln (L/d), D_{tube} is given by[29]

$$D_{tube} = kT/2\pi\eta L \quad (10)$$

Hence

$$\tau_R = \pi\eta L^3/kT \quad (11)$$

Note that D_{tube} and τ_R are independent of the flexibility of the chain. Equations 10 and 11 apply to flexible, wormlike, and rodlike polymer melts. After a time τ_R the chain has diffused, on average, in three-dimensional space just over its own end-to-end vector. Therefore

$$D_s = \langle h^2\rangle/6\tau_R \quad (12)$$

Chain flexibility enters the evaluation of D_s through the P dependence of $\langle h^2\rangle$. Assuming ideal chain behavior also in the melt (eq 2), one obtains

$$D_s = \frac{kT}{3\pi\eta L}\frac{P}{L} \quad (13)$$

which is $2P/a$ times larger than D_s for completely flexible chains.

In the semidilute regime $c^* < c \ll 1$ a modified reptation model has been proposed[6] for *flexible* chains: At distances larger than a, but too short for a segment to "sense" the presence of neighboring chains, the test chain is assumed to take the same conformations as in dilute solutions. Then a concentration-dependent intermolecular correlation length ξ is introduced and the chain conformation at long distances ($\gg\xi$) is described by a random sequence of objects (so-called "blobs") of size ξ. This ideal chain of blobs, which has a primitive chain length $L' = N_{blob}\xi < L$, performs reptation inside the "melt" of other ideal blob chains. Therefore eq 9–11 are applied with L replaced by L'. As a simple approach, the effective local viscosity in eq 11 is set equal to the solvent viscosity η_0. The number of blobs per chain, N_{blob}, equals N/g, where g is the number of chain segments inside a blob. g is related to ξ by the random walk relation.[6] This implies of course that $\xi \gg a$, but the situation should be very similar for wormlike chains as long as $\xi \gg 2P$. We then put, on average

$$\xi^2 = 2Pag \quad (14)$$

This gives $L' = 2PL/\xi$ and $\langle h^2\rangle = L'\xi = 2PL$. It then follows from eq 12 that

$$D_s = \frac{kT}{6\pi\eta_0}\frac{\xi^3}{(2PL)^2} \quad (15)$$

The c dependence of ξ is obtained by the requirement that (i) ξ should be independent of the chain length L inside the semidilute regime and (ii) ξ should equal R_g at c^*. A scaling form satisfying (ii) is

$$\xi = R_g(c^*/c)^\nu \quad (16)$$

Using eq 2 and 8 one obtains from (i) $\nu = 1$ and hence

$$\xi = 3m/Pc \quad (17)$$

Inserting ξ (eq 17) into eq 15, we find for D_s in the semidilute regime above c^*

$$D_s = \frac{9kT}{8\pi\eta_0}\frac{1}{P^5L^2}(m/c)^3 \quad (18)$$

This formula has the same length exponent (−2) as the widely known[6] relation $D_s \simeq (kT/\eta_0 a)N^{-2}c^{-7/4}$ derived for flexible chains from the blob picture. The different c dependence stems from the use of the ideal length exponent (1/2) for R_g instead of the Flory exponent (3/5). The effect of chain stiffness enters through a factor of order $d^6/aP^5 \simeq (a/P)^5$, which is a very small number for typical wormlike chains (e.g., $\simeq 10^{-8}$ for $P/a = 45$). D_s thus appears very sensitive to chain stiffness in the semidilute regime. Note that this semidilute regime characterized by $\xi > 2P$ should always exist above c^*, as $2P < R_g$ by definition (eq 2) and $\xi = R_g$ at c^*.

With increasing c, however, ξ decreases, whereas P supposedly stays constant. One might therefore expect another regime to appear above a new crossover concentration c_c characterized by $\xi(c_c) = 2P$. We shall call this regime "concentrated"—despite of the fact that for typical wormlike polymers c_c may be much smaller than the bulk polymer density—because the reptation mechanism expected in this regime is rather similar to the one for melts outlined above: When $\xi < 2P$ the chain conformation at length scales $\leq \xi$ can no longer be modeled by a random walk and hence the blob picture breaks down. The test chain rather behaves like a smoothly bending rod at scale ξ and therefore should reptate essentially by curvilinear diffusion along its contour, i.e., inside a tube of cross section ξ^2 and length L. In contrast to melts, however, the friction is essentially solvent friction as long as the polymer volume fraction is much smaller than 1, or equivalently, $\xi \gg a$. Let us estimate c_c and D_s in the concentrated regime. Setting $\xi \equiv 2P$ in eq 17 gives

$$c_c = 3m/2P^2 \quad (19)$$

The reptation time is the one for curvilinear diffusion (eq 11) with η being replaced by η_0. With $\langle h^2\rangle = 2PL$ we obtain from eq 12

$$D_s = \frac{kT}{3\pi\eta_0}\frac{P}{L^2} = \frac{2P}{3L}D_{tube} \quad (20)$$

Since the chain is constrained to curvilinear diffusion, like in melts of wormlike chains, eq 20 is identical with eq 13, except for the local viscosity. Equation 20 gives the same length exponent as in the semidilute regime, but there is *no* concentration dependence of D_s, in strong contrast to eq 18. As long as the chains are sufficiently confined to guaranty curvilinear diffusion, but polymer–polymer friction is still negligible, the actual (concentration dependent) ξ value is not relevant for evaluating D_s in the concentrated regime. By inserting c_c (eq 19) into eq 18, we see that the expressions for D_s of the semidilute and concentrated regimes match c_c.

The above relations have been derived (i) for long chains ($P \ll L$) as the limiting form $R_g \propto L^{1/2}$ was used and (ii) by omitting logarithmic corrections for D_{tube}. Doi[14] and Semenov[15] have both given relations for D_s in the concentrated regime over the full L range from rods ($L \ll P$) to worms ($L \gg P$). In the high-L limit the results of Doi and of Semenov are identical with the right-hand side of eq 20. They also mutually agree in the low-L limit, which is not considered in this paper. At finite L/P the analytic expressions of $D_s(L/P, D_{tube})$ given in ref 14 and 15 differ somewhat. In the range of interest covered by our experimental data the difference between these expressions[14,15] for finite L/P and the limiting form (eq 20) are on the order of at most $\simeq 8\%$ for the lowest L/P value, which is 10. Considering our experimental uncertainties in D_s (see below) and the theoretical uncertainties in the numerical coefficients inherent to scaling, it

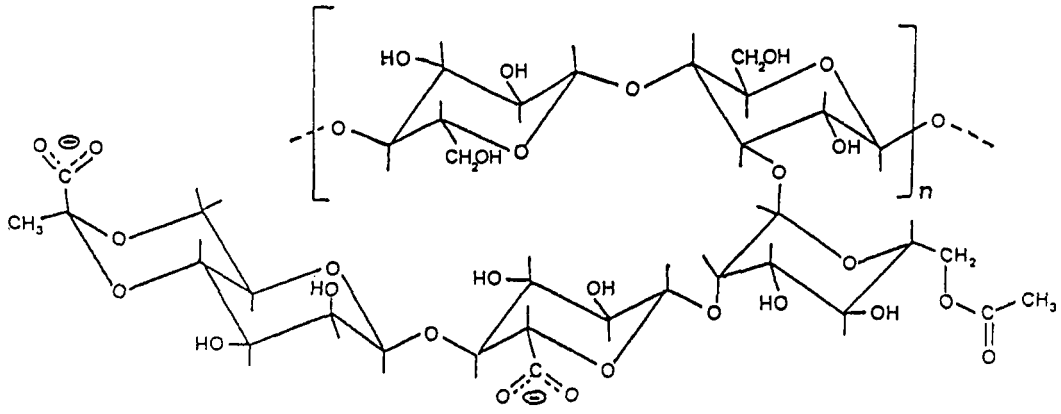

Figure 1. Schematic representation of the polysaccharide xanthan.

seems not meaningful to include these (minor) corrections in the comparison between theory and experiment.

The expression (eq 10) for D_{tube} is approximate. Using a model of aligned touching spheres, Kirkwood et al.[29] have calculated the self-diffusion constant of a long thin rod (of length L and diameter d) parallel to its long axis:

$$D_{\parallel} = \frac{kT}{2\pi\eta_0 L} \ln (L/d) \tag{21}$$

It appears physically appealing to use this expression also for the self-diffusion constant D_{tube} of a wormlike chain along its contour in the melt and in the concentrated regime. This provides a correction term ln (L/d) to the right-hand sides of eq 13 and 20. Semenov,[15] on the other hand, applies Kirkwood's result to individual Kuhn segments and calculates D_{tube} by summing the segment friction coefficients $4\pi\eta_0 P/\ln (2P/d)$ over the chain. This gives

$$D_{tube} = \frac{kT}{2\pi\eta_0 L} \ln (2P/d) \tag{22}$$

The resulting correction ln $(2P/d)$ in eq 13 and 20 becomes physically meaningless when approaching the rod limit ($P > L$), unlike the correction ln (L/d).[8,14] The evaluation of the corresponding correction in the semidilute regime depends on the model for the effective hydrodynamic diameter ξ_h of the blob chain. With $\xi_h = \xi$ as a first guess the correction to eq 18 would be ln (L'/ξ) = ln $(2PL/\xi^2)$. This can be considered as a lower bound, since ξ_h should be smaller than ξ because of penetration of solvent flow inside the blobs. This approximation becomes meaningless for $\xi \to 2P$, because, at c_c, the hydrodynamic diameter ξ_h for the curvilinear diffusion should not be of order $2P$ but rather of order d. The correction term in eq 18 should cross over to ln (L/d) near c_c; thus, ln (L/d) may be considered an upper bound.

Samples

Xanthan is an extracellular polysaccharide produced by the bacterium Xanthomonas campestris. The backbone is a $\beta(1-4)$-linked D-glucopyranose chain, as in cellulose, but with a trisaccharide side chain, attached at C3 to alternate glucose residues (Figure 1). This side chain consists of a partially acetylated mannose residue, a glucuronic acid, and a pyruvate ketal linked to a terminal mannose residue. Therefore, xanthan is a polyelectrolyte and the experiments reported here were performed in 0.1 N NaCl to prevent electrolyte effects on the length scale P. The side chains give a semirigid character to the main chain.

The starting product for sample preparation was kindly provided by Shell. Its initial molecular weight was 9.4×10^6 as determined by conventional elastic low-angle light scattering. Contents in pyruvic and acetyl groups were 40% and 70%, respectively. Fluorescent derivatives were prepared by isocyanide coupling of fluoresceinamine to the carbonyl groups of xanthan. 5-aminofluorescein, acetaldehyde, and cyclohexyl isocyanide were used as reagents, following the procedure described by Holzwarth.[30] The labeled polysaccharide was purified by several cycles of precipitation by ethanol, washed, and dried at 30 °C under reduced pressure. The degree of fluorescent labeling was 2.6×10^{-2} per disaccharide of the main chain (equivalent to one fluorescent group per 38.5 nm), measured by optical absorption spectroscopy.

From the initial labeled product, samples of different molecular weight were prepared by sonication.[30] The ultrasound generated by a Branson Model B12 (150 W) was transmitted into a continuous flow cell with a microtip. By adjusting the flow rate and the number of flow cycles, samples of various molecular weights were obtained. Subsequently the solutions were filtered through a 0.22-μm pore membrane, brought to 1 M NaCl, and precipitated in 95% ethanol. Samples were washed and dried as described earlier.[31]

Weight-average molecular weights and their distributions were determined by gel permeation chromatography on 1 × 6000 and 1 × 4000 TSK PW columns of 60-cm length by using a differential refractometer, an online low-angle light scattering apparatus, and a fluorescence detector. The elution was performed at 25 °C with 0.1 M $NaNO_3$ in the presence of 0.2 g/L of NaN_3 as bactericide and 1% ethylene glycol to prevent adsorption. By this method and with use of optical rotation, viscosity, and ^1H NMR measurements, we made sure that the ultrasonic and fixation procedure did not yield substitution of the side chains or affect the degree of labeling. The main characteristics of the labeled samples are given in Table I. The polydispersity appears reasonably low.

Experimental Section

The self-diffusion coefficient of fluorescein-labeled xanthan molecules was measured by a fringe pattern fluorescence bleaching technique similar to the one described by Davoust et al.[22] The light beam of an etalon-stabilized monomode Ar laser (1 W at λ = 488 nm) was split and the two beams crossed in the sample cell providing illumination in a deep interference fringe pattern. The fringe spacing $2\pi/q$ set by the crossing angle θ, $q = 4\pi/\lambda \sin \theta/2$, ranged from 8 to 58 μm, defining the diffusion distance. Fluorescence bleaching of the labeled polymers in the illuminated fringes was obtained by producing a 1-s full-inten-

Table I
Main Characteristics of Samples[a]

$\bar{M}_w$, 10^6	$[\eta]$, cm^3/g	I
9.4	15200	
3.8	4500	
1.9	2400	1.4
0.99	1140	1.18
0.45	405	1.22

[a] $\bar{M}_w$ = weight-average molecular weight; $[\eta]$ = intrinsic viscosity; I = polydispersity index.

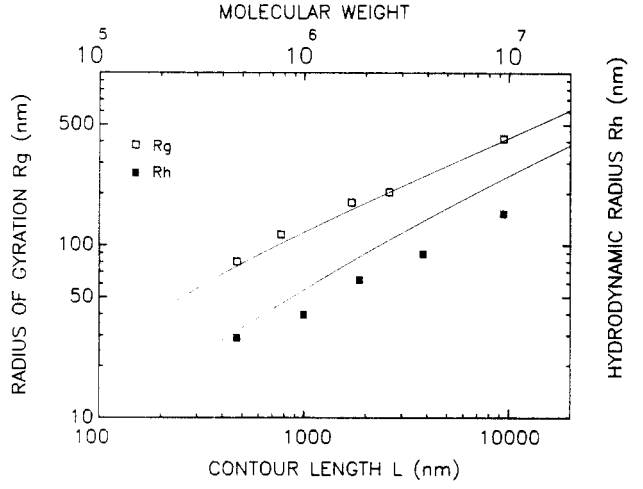

Figure 2. Molecular weight dependence (in the dilute regime) of R_g in comparison with eq 1, 3, and 5, upper line, and of R_h in comparison with the same theoretical expression multiplied by ζ (eq 7), lower line; $T \simeq 22$ °C.

sity bleach pulse by mechanically switching a depolarizer into the beam at a location between nearly crossed polarizers. The decay of the amplitude of the fringe pattern of concentration of fluorescent polymers after bleaching was detected by modulation of the illuminating fringe position using a piezoelectrically modulated mirror and lock-in detection of the emerging fluorescence. Nonpreaveraged data were fitted to a single exponential $\exp(-t/\tau)$, D_s was calculated from $1/\tau = D_s q^2$, and D_s values from several shots were averaged.

Most of the measurements were performed on samples with *all* molecules weakly labeled. In order to verify that this procedure provides a correct measure of D_s, data were also taken in the semidilute and concentrated regimes, respectively, of *unlabeled* xanthan, keeping the concentration of labeled polymer below c^*.[32] The D_s values (of the labeled species) obtained in the unlabeled environment agree—within experimental error—with the values in the labeled environment.

R_g values were obtained in the dilute regime from angle-dependent static light scattering using Zimm plots.

Results

1. Dilute Solutions. Figure 2 shows the R_g values as obtained from static light scattering as a function of molecular weight (or chain length L). The upper continuous line is a fit to eq 1 and 3–5, using $d_e = 2.8$ nm.[26] The resulting persistence length is $P = 45$ nm. Note that relation 3 becomes very close to eq 2 (exponent 1/2) for $\bar{M}_w \geq 10^6$. Figure 3 shows the concentration dependence of D_s for various molecular weights. In the dilute regime D_s is found independent of c. Figure 2 also gives the experimental values of the hydrodynamic radius R_h obtained from the average D_s values in the dilute regime and using eq 6. The L dependence of R_h is very similar to the L dependence of R_g, but the absolute R_h values are substantially smaller than R_g, indicating the strong penetration of solvent flow through the polymer chains ($\zeta \simeq 0.35 \pm 0.12$). For comparison we plot the L dependence of R_h as calculated from eq 7 using R_g from eq 1 and 3–5 with $P = 45$ nm and $d = 1.1$ nm.[33] The experimental ζ values appear somewhat smaller than this theoretical evaluation, in particular at large L. The reason for this remains unclear to us. Notwithstanding, it seems appropriate to describe the translational diffusion of noninteracting xanthan molecules by a wormlike persistent chain model with (weak) coil expansion due to excluded volume between segments.

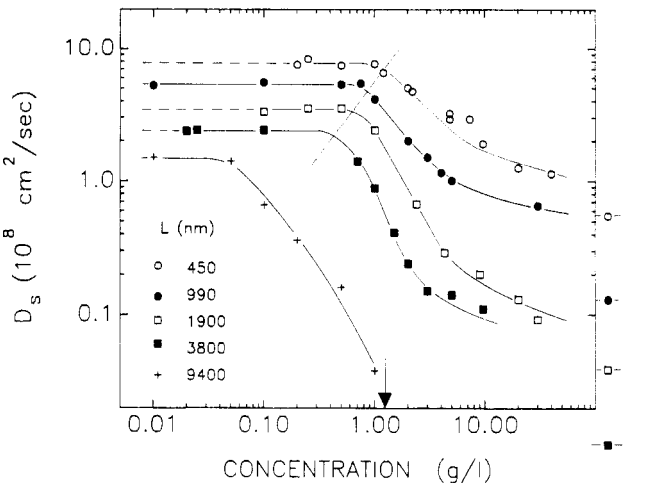

Figure 3. Self-diffusion constant D_s of xanthan at various contour lengths L in aqueous solution at 0.1 M NaCl ionic strength, $T \simeq 22$ °C. Continuous lines are guides to the eye. Dashed line: c^* calculated from eq 8 and 2. Also indicated are c_c from eq 19 and—outside the frame—the limiting values of D_s in the concentrated regime calculated from eq 20 and 2.

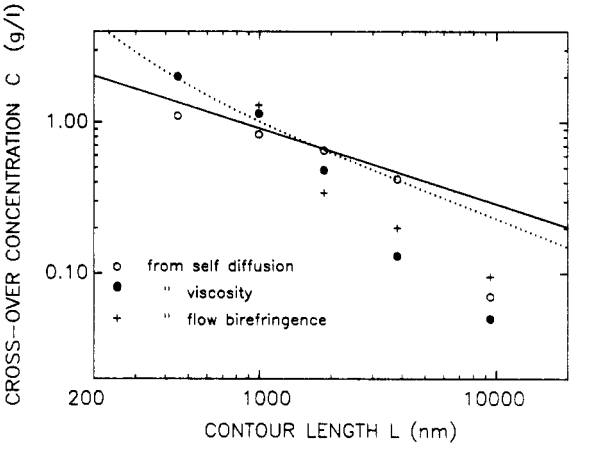

Figure 4. Crossover concentration between the dilute and semidilute regime estimated from different experiments and calculated for a wormlike chain in the Gaussian limit (—), eq 2 and 8, and with excluded-volume correction (· · ·), eq 1, 3–5, and 8; $P = 45$ nm, $d_e = 2.8$ nm.

2. Semidilute Solutions. For increasing concentration, the self-diffusion constant becomes progressively smaller for all molecular weights (Figure 3). The onset of the slowing down, however, depends on L. This is more clearly shown in Figure 4 where the experimental crossover concentrations c^* are plotted. We have deduced c^* from the crossing points of linear extrapolations of the c dependence of D_s, of the flow birefringence, and of the viscosity. This evaluation of c^* is subject to substantial experimental error. The dotted or continuous line in Figure 4 corresponds to the theoretical estimation (eq 8) using for R_g the full expression (eq 1, 3–5) or the approximate form (eq 2), respectively. Both estimations of c^* seem to provide the correct order of magnitude, but the L depen-

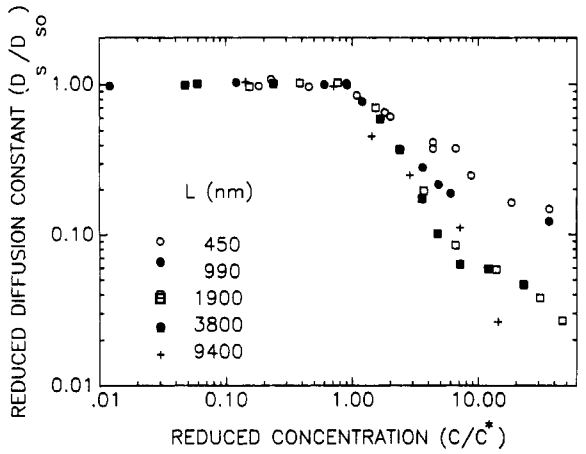

Figure 5. Self-diffusion constant normalized to the average value D_{so} measured in the dilute regime versus concentration in units of the experimental crossover concentration c^* (from {O} in Figure 4).

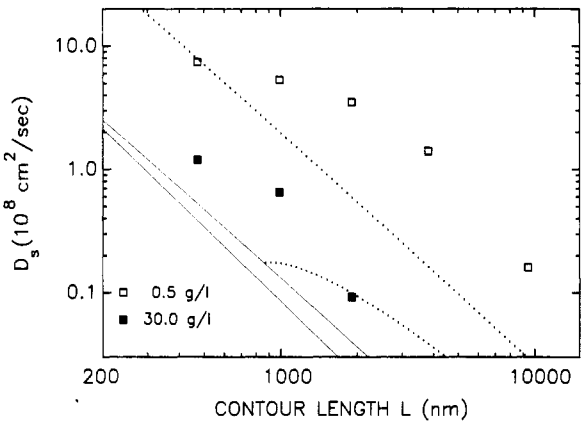

Figure 6. Length dependence of the self-diffusion constant measured in the semidilute regime (c = 0.5 g/L) and in the concentrated regime (c = 30.0 g/L), in comparison with the scaling estimations: (···) Equation 18, semidilute, with correction terms ln (L/d) (upper curve) and ln $(2PL/\xi^2)$ (lower curve). (—) Equation 20, concentrated, with correction terms ln (L/d) (upper curve) and ln $(2P/d)$ (lower curve). P = 45 nm, d = 1.1 nm.

dence appears somewhat too small, as particularly evident from the data at the highest molecular weights. The dashed line in Figure 3 represents eq 8 and eq 2 with P = 45 nm. It connects the calculated c^* values when plotted on the corresponding horizontal lines through the dilute solution D_s values for each L. It locates reasonably well the crossover from the dilute to the semidilute regime.

Above c^* the observed slowing down of the self-diffusion appears more pronounced at higher molecular weights, but when all the data are plotted on a reduced scale (Figure 5), i.e., log D_s/D_{so} versus log c/c^* (D_{so} being the average D_s value in the dilute regime), a master curve may be obtained up to $c/c^* \simeq 2$. The data scale with c/c^*, as assumed in the derivation of eq 18. However, the slope of this plot in the semidilute regime remains substantially smaller than −3, presumably because a new crossover into a less c-dependent regime (see below) sets in before the limiting behavior is reached. This may be better seen in Figure 3. The c range where a sample can possibly be considered in the semidilute regime appears very narrow, in particular at low L. In Figure 6 we plot the L dependence of D_s at 0.5 g/L. The observed increase of the L dependence with increasing L is consistent with the existence of a narrow semidilute regime broadening with increasing L. Also given in this figure are the predicted D_s values calculated from eq 18 by using the logarithmic corrections ln (L/d) (upper bound) and ln $(2PL/\xi^2)$ (lower bound). It is not surprising, because of the narrowness of the semidilute regime, that the data are located well above both scaling estimations, but considering the strong P and c dependence of D_s in eq 18, the agreement in order of magnitude seems worth mentioning. We also notice that the ξ values calculated from eq 17 range from 222 nm at c = 0.5 g/L to 92.6 nm at c = 1.2 g/L, which is larger than P and smaller than R_g, as required by the model.

3. "Concentrated" Solutions. At concentrations of around 2–4 g/L the slowing down of D_s with increasing c seems to become weaker (Figure 3). In contrast to c^* this new crossover concentration appears essentially molecular weight *independent*, as predicted by eq 19. Putting P = 45 nm into eq 19 gives in fact c_c = 1.23 g/L, as indicated by the vertical arrow in Figure 3, which is in fair agreement with the experimental crossover range. This suggests that at higher c, the concentrated regime characterized by curvilinear diffusion is approached. Unfortunately the measurements cannot be extended to higher concentrations because of the appearance of a lyotropic liquid-crystalline phase and the very elevated viscosity of the highest molecular weight samples. Hence the c *in*dependence of D_s predicted by eq 20 cannot be unambiguously observed. It remains unclear to us whether this is because the limiting regime cannot be reached in principle or whether c-dependent effects neglected in eq 20 such as monomer–monomer friction or chain end effects become important. Our observation that the translational diffusion of free fluorescein molecules (D_s = (2.8 ± 0.2) × 10^{-6} cm^2/s at c = 0) appears—within our experimental accuracy—rather independent of the presence of polymer (D_s = (3.2 ± 0.3) × 10^{-6} cm^2/s at c = 21.7 g/L) would argue that the monomer–monomer friction effect should be small. The points outside the right-hand scale of Figure 3 and the upper continuous line in Figure 6 give the limiting plateau values of D_s as calculated from eq 20 with P = 45 nm, d = 1.1 nm, and the correction ln (L/d).[14] The same expression, but with ln $(2P/d)$ instead,[15] is given as the lower continuous line in Figure 6. The quantitative agreement between both models[14,15] and the experimental data appears satisfactory, if one admits the uncertainties of numerical coefficients and that the limiting regime may not be reached experimentally with this polymer system. In addition, we have verified[32] that in the concentrated regime the short polymer chains of a given length diffuse at a rate corresponding to their own length L, irrespective of the length of the surrounding (longer) polymer chains, as required by the reptation model.

In conclusion, we have measured the self-diffusion coefficient of the wormlike polysaccharide xanthan over a wide range of concentrations for various molecular weights. Our data reveal, besides the dilute and semidilute regime, the existence of a new "concentrated" regime characteristic of wormlike chains at concentrations where the intermolecular correlation length ξ becomes smaller than the persistence length P. Because the reptation process in this regime resembles the one in melts, translational diffusion can be expected to become concentration independent. Simple scaling arguments result in expressions for D_s, c^*, and c_c that are consistent with the main trends in the data as a function of concentration and chain length and, in addition, provide a fair estimate for the order of magnitude of the self-diffusion constant and of the crossover concentrations.

Acknowledgment. We acknowledge very fruitful discussions with J. F. Joanny, R. Klein, H. Frisch, and M. Milas.

References and Notes

(1) Schaefer, D. W.; Han, C. C. In *Dynamic Light Scattering and Velocimetry. Applications of Photon Correlation Spectroscopy*: Pecora, R, Ed.; Plenum Press: New York, 1984.
(2) Tirrell, M. *Rubber Chem. Technol.* **1984**, *57*, 523.
(3) Graesley, W. W. *Adv. Polym. Sci.* **1974**, *16*, 1.
(4) de Gennes, P.-G. *J. Chem. Phys.* **1971**, *55*, 572.
(5) Doi, M.; Edwards, S. F. *J. Chem. Soc., Faraday Trans. 2* **1978**, *74*, 1789, 1802, 1818.
(6) de Gennes, P.-G. *Scaling Concepts in Polymer Physics*; Cornell University Press: London, 1979.
(7) Doi, M.; Edwards, S. F. *The Theory of Polymer Dynamics*; Int. Ser. Monographs. Phys. 73; Clarendon Press: Oxford, 1982.
(8) Doi, M.; Edwards, S. F. *J. Chem. Soc., Faraday Trans. 2* **1978**, *74*, 560.
(9) Edwards, S. F.; Evans, K. F. *J. Chem. Soc., Faraday Trans. 2* **1982**, *78*, 113.
(10) Frenkel, D.; Maguire, J. F. *Phys. Rev. Lett.* **1981**, *47*, 1025.
(11) Doi, M.; Yamamoto, I.; Kano, F. *J. Phys. Soc. Jpn.* **1985**, *53*, 3000.
(12) Schaefer, D. W.; Joanny, J. F.; Pincus, P. *Macromolecules* **1980**, *13*, 1280.
(13) Odijk, T. *Macromolecules* **1980**, *16*, 1340.
(14) Doi, M. *J. Polym. Sci., Polym. Symp.* **1985**, *73*, 93.
(15) Semenov, A. *J. Chem. Soc., Faraday Trans. 2* **1986**, *82*, 317.
(16) Zero, K. M.; Pecora, R. *Macromolecules* **1982**, *15*, 87.
(17) Russo, P. S. *Macromolecules* **1985**, *18*, 2733.
(18) Pecora, R. *J. Polym. Sci., Polym. Symp.* **1985**, *73*, 83.
(19) Fujime, S.; Takasaki-Oshita, M.; Maeda, T. *Macromolecules* **1987**, *20*, 1292.
(20) Coriello, T.; Burchard, W.; Dentini, M.; Crescenzi, V. *Macromolecules* **1987**, *20*, 1102.
(21) Léger, L., private communication.
(22) Davoust, J.; Devaux, P. F.; Léger, L. *EMBO J.* **1982**, *1*, 1233.
(23) Benoit, H.; Doty, P. *J. Phys. Chem.* **1953**, *57*, 958.
(24) Yamakawa, H. *Modern Theory of Polymer Solutions*; Harper & Row: New York, 1971.
(25) Odijk, T.; Houwaart, A. *J. Polym. Sci., Polym. Phys. Ed.* **1978**, *16*, 627.
(26) The diameter d_e for the determination of the excluded volume was calculated for an ionic strength of 0.1 M NaCl by using the theory of: Skolnick, J.; Fixman, M. *Macromolecules* **1977**, *10*, 944.
(27) Flory, P. *Principles of Polymer Chemistry*; Cornell University Press: Ithaca, NY, 1971.
(28) Berry, G. C. *J. Polym. Sci., Polym. Phys. Ed.* **1988**, *B26*, 1137.
(29) Riseman, J.; Kirkwood, J. G. *J. Chem. Phys.* **1950**, *18*, 512. Kirkwood, J. K.; Auer, P. L. *J. Chem. Phys.* **1951**, *19*, 281.
(30) Holzwarth, G. *Carbohydr. Res.* **1978**, *66*, 173.
(31) Milas, M.; Rinaudo, M.; Tinland, B. *Carbohydr. Polym.* **1986**, *6*, 95.
(32) Labeled polymers with L = 990 nm at c_1 = 0.1 g/L were mixed into unlabeled polymers with L = 770, 1700, and 2600 nm at two different concentrations (c_u : 4.5 g/L and c_u = 27 g/L). We obtain $D_s \simeq 1 \times 10^{-8}$ cm^2/s for all samples at c_u = 4.5 g/L and $D_s \simeq 0.7 \times 10^{-8}$ cm^2/s for all samples at c_u = 27 g/L.
(33) Estimation of the hydrodynamic diameter of xanthan (c.f., Figure 1) appears difficult to us. In a first approximation we use the geometric diameter $d \simeq 1.1$ nm as calculated from $m = 1.67 \times 10^{-14}$ g/cm and a density of 1.62 g/cm^3.

Registry No. Xanthan, 11138-66-2.

Chain Stiffness and Excluded-Volume Effects in Dilute Polymer Solutions. Poly(isophthaloyl-*trans*-2,5-dimethylpiperazine)

Tooru Kitagawa, Jiro Sadanobu,† and Takashi Norisuye*

Department of Macromolecular Science, Osaka University, Toyonaka, Osaka 560, Japan.
Received May 1, 1989; Revised Manuscript Received July 3, 1989

ABSTRACT: Small-angle X-ray scattering, light scattering, and viscosity measurements were made on 18 sharp fractions of poly(isophthaloyl-*trans*-2,5-dimethylpiperazine) (PIDP), a flexible polyamide, ranging in weight-average molecular weight M_w from 2.6×10^3 to 2.4×10^6, with *N*-methyl-2-pyrrolidone (NMP) at 25 °C as the solvent. Both gyration radius and intrinsic viscosity data showed PIDP in NMP to be essentially unperturbed below $M_w \sim 10^4$ and perturbed above it by volume effect. When modeled by Kratky and Porod's wormlike chain, the unperturbed PIDP chain was characterized by a persistence length of 1.2 nm and a molar mass per unit contour length of 310 nm^{-1}. It was found that the combination of the Yamakawa–Stockmayer perturbation theory for the radius expansion factor of a wormlike chain and the Domb–Barrett equation for a flexible chain accurately describes the dimensional behavior of PIDP in NMP over the entire range of M_w studied.

Excluded-volume effects in dilute polymer solutions have been discussed mostly with theories[1,2] formulated for perfectly flexible chains in which the probability of segment collision vanishes only in the limit of zero chain length. In an actual polymer molecule, flexible or stiff, the probability must become zero at a certain nonzero chain length.[3,4] Thus we should treat even a flexible polymer as semiflexible to explain dilute-solution properties of linear polymers over a broad range of chain stiffness or chain length. In experimental studies on flexible polymers, measured properties, especially radii of gyration $\langle S^2 \rangle^{1/2}$, without excluded volume at low molecular weights may be analyzed with a relevant model for semiflexible polymers, and thereby volume effects can be estimated separately from stiffness effects. Such attempts were made by Tsuji et al.[5] for Bisphenol A polycarbonate and by Huber et al.[6] for polystyrene with Kratky and Porod's wormlike chain[7] as the model, but the $\langle S^2 \rangle$ data obtained were not extensive enough to allow quantitative discussions on volume effects.

The present work is concerned with a similar attempt made for poly(isophthaloyl-*trans*-2,5-dimethylpiperazine) (PIDP), a polyamide consisting of repeating units shown in Figure 1. We made small-angle X-ray scatter-

† Present address: Products Development Research Laboratories, Teijin Co., Iwakuni 740, Japan.

0024-9297/90/2223-0602$02.50/0